Engineered Science
DOI: https://dx.doi.org/10.30919/es1460

Hydrothermal Synthesis and Photocatalytic Performance of Zinc Oxysulfide for Hydrogen Evolution

Tolagay Duisebayev,[1] Muhammad Abdullah,[1] Yerbolat Tezekbay,[1] Mergen Zhazitov,[1] Nazerke Kydyrbay,[1] Nurxat Nuraje[1, 2] and Olzat Toktarbaiuly[1,*]

Abstract

The global shift toward sustainable energy requires the development of efficient hydrogen production. In this work, zinc oxysulfide (ZnOS) photocatalysts were produced by the hydrothermal method, where careful control of precursor ratios, reaction temperatures, and annealing conditions enabled a precise tuning of structural and optical properties. Experimental characterization also demonstrated that annealing transforms initially rough, spherical ZnOS particles into smoother, highly crystalline forms, as evidenced in scanning electron microscope (SEM) and X-ray diffraction (XRD). Ultra-violet visible (UV-Vis) absorption spectroscopy reveals significant enhancements in visible light absorption within the 350 nm range, indicating changes in electronic structures and increased charge separation. Ultimately, the successful deposition of ZnOS films onto glass substrates demonstrates the scalability and adaptability of our synthesis route for optoelectronic applications. This work offers new insights into the behavior of synthesis parameters and photocatalytic performance, suggesting a promising path forward for the preparation of high-performance, tunable ZnOS materials for sustainable hydrogen production.

Keywords: Renewable energy; Tunable band gaps; Improved charge separation; Visible light absorption.
Received: 04 March 2025; Revised: 17 March 2025; Accepted: 24 March 2025.
Article type: Research article.

1. Introduction

The global transition towards clean energy systems is in dire need of hydrogen production technologies that are clean and efficient. Hydrogen, which can significantly reduce carbon emissions and help halt global warming, has emerged as a crucial energy carrier. The annual global production of hydrogen already stands at 75 million tons, of which nearly 45% is produced through natural gas reforming, indicating a significant reliance on fossil fuels.[1] Although hydrogen demand is expected to grow at a rate of 6% annually, driven by applications in transportation, industry, and electricity generation, there is an urgent need for sustainable production methods.[2]

Among the materials researched for hydrogen generation, zinc compound-based materials, such as zinc oxysulfide (ZnOS), are of significant interest. They are rich, non-toxic, and possess properties that can be tuned to be used as photocatalytic water splitters and photodetectors.

Coupling high-temperature and high-pressure environments with hydrothermal reactions has yielded ZnOS with novel structure and functionality characteristics.[3] Synthesis conditions, specifically pressure and temperature, play a crucial role in determining the crystal structures of ZnOS, including the wurtzite and zinc blende phases. Synthesis conditions also favor the generation of mixed oxysulfide phases, where zinc oxide (ZnO) and zinc sulfide (ZnS) become mutually soluble, thereby stabilizing and enhancing the material's functionality.[3] The nano-thin film, which provides a smooth and homogeneous nanoparticle morphology of ZnOS, is particularly valuable for photocatalytic applications. Its increased surface area and better efficiency in charge separation are directly equivalent to enhanced photocatalytic performance.[4] Compared with typical photocatalysts like titanium oxide (TiO_2) and pure ZnO, ZnOS heterostructures exhibit enhanced charge separation and visible light absorption and are highly effective in photocatalytic hydrogen evolution. Heterostructures of ZnOS exhibit great water splitting under visible light at a hydrogen evolution rate as much as 788.7154 μmol g^{-1} h^{-1}.

[1] *Renewable Energy Laboratory, National Laboratory Astana (NLA), Nazarbayev University, Kabanbay Batyr 53, Astana, 010000, Kazakhstan*
[2] *Department of Chemical & Materials Engineering, School of Engineering & Digital Science, Nazarbayev University, Astana, 010000, Kazakhstan*
**Email:* olzat.toktarbaiuly@nu.edu.kz (O. Toktarbaiuly)

Precise control over ZnOS properties is achievable due to the hydrothermal growth mechanism, and doping with trithiocyanuric acid enhances photocatalytic activity by improving charge transfer and separation.[5] Recent advances in synthesis methods have enabled more effective control of ZnOS composition and structure, and even further advancements are feasible. High-pressure solvothermal treatments have been investigated for the development of novel ZnOS morphologies and phases, aiming to enhance their performance in hydrogen-related applications.[6,7] The efficiency of ZnOS in photocatalytic water splitting depends mainly on its optical and structural properties, such as band gaps and charge separation efficiency, which are crucial in attaining optimum hydrogen yield rates.[8] ZnO thin films are extremely suitable for applications such as solar cells and photo detectors, offering efficient charge transport and light absorption. Control of the optical and electrical properties of ZnOS thin films becomes achievable, opening new areas for their application in the energy sector. Improvement regarding compositional homogeneity on wider substrates, stability under extended application, and production scale-up while preserving functionality must be undertaken.[9] Despite these challenges, ZnOS materials synthesized through hydrothermal processes hold tremendous promise for hydrogen generation and other energy applications. Further research is needed to optimize the synthesis parameters, including temperature, pressure, and chemical composition, to realize the potential of ZnOS fully.[10,11]

The climate implications of using fossil fuels underscore the urgent need to transition to renewable energy sources. Hydrogen is a clean fuel that offers a promising future, as its combustion releases only water vapor, thereby reducing greenhouse gas emissions.[12] However, conventional means of hydrogen generation, such as steam methane reforming and water electrolysis, are constrained by cost, efficiency, and scale.[13-16] Metal oxide semiconductors, particularly ZnO, hold potential for photocatalysis since they are inexpensive, chemically stable, and have good electronic properties.[12] However, the wide band gaps of these materials (3.1-3.4 eV) limit their light absorption primarily to the ultraviolet (UV) region, which accounts for only about 5% of the solar spectrum. To utilize the more abundant visible light (approximately 50% of the solar spectrum), researchers have been exploring methods such as doping, defect engineering, and the formation of heterojunctions.[10,17] Unfortunately, such strategies lead to problems of dopant precipitation, poor solubility, and elevated electron–hole recombination rates, which limit photocatalytic efficiency.[17,18]

One approach is to stabilize high-pressure phases in metal oxides using severe plastic deformation techniques, specifically high-pressure torsion (HPT). HPT consists of the concurrent imposition of high pressure and enormous plastic strain that alters the thermodynamic status to stabilize naturally unstable phases at atmospheric conditions.[19] For instance, HPT processing has successfully transformed the customary wurtzite structure of ZnO into a rocksalt phase at high pressure, resulting in a narrower band gap and enhanced visible-light absorption and photocatalytic activity.[20-22] The ZnO–ZnS system has been investigated to prepare zinc oxysulfide materials that combine the favorable properties of ZnO and ZnS. The mixed compounds offer tunable band gaps, making them suitable for applications in photovoltaics and photocatalysis.[3,23] Hydrothermal synthesis methods have been employed to synthesize uniform semiconductor powders of high photocatalytic activity. Hybrid methods involving hydrothermal synthesis and calcination have also been demonstrated to synthesize ZnOS heterostructures with enhanced charge separation and visible light adsorption.[24]

The flexibility of ZnO-based semiconductors is evident in their applications in transistors and optoelectronic devices.[25] For photocatalytic applications, the primary challenge is overcoming the inherent disadvantage of the wide band gap. The phase transformation of ZnO into those with narrower band gaps, such as the high-pressure rocksalt phase, has substantially enhanced visible-light-driven photocatalytic hydrogen evolution.[21,22] The feasibility of wurtzite ZnO converting into a novel triclinic nanoporous phase with increased proton conductivity via hydrothermal treatment, resulting in improved photocatalytic activity.[17]

Research on the interaction between hydrogen and defects in ZnO nanoparticles indicated that oxygen vacancies and other defects play a key role in manipulating the electronic structure and photocatalytic activity.[18,26] Spectroscopic measurements have also confirmed that ZnO nanorods are stable under shock wave conditions, as required for applications in hostile environments, such as aerospace.[26]

The extensive optical investigation has provided accurate data on the vibrational modes and electronic structures of ZnO in its wurtzite and high-pressure rock salt forms.[27,28] In situ synchrotron high-pressure X-ray diffraction experiments also confirm that the rock salt phase can be stabilized under room conditions after HPT processing.[29] Theoretical research confirms these experimental findings by indicating that the phase transformation from wurtzite to rock salt ZnO results in a narrowed band gap due to a shift from mixed ionic-covalent to predominantly ionic bonding.[30] Levitas and Javanbakht provided a comprehensive study of phase transformations in nanograin materials under high pressure and plastic shear,[31] explaining the nanoscale mechanisms for the stabilization of high-pressure phases at room temperature. More recent studies by Razavi-Khosroshahi and Fuji have further demonstrated that such high-pressure phases, when stabilized using HPT, exhibit improved photocatalytic properties.[20]

Severe plastic deformation, as a means of band gap engineering, has been taken to the next level by Razavi-Khosroshahi *et al*.,[22] whose findings have proven that this process can effectively reduce the band gap of metal oxides and ceramics, thereby advancing their solar energy harvesting ability. Notably, stabilization of the rocksalt high-pressure phase in ZnO reduces its band gap to a minimum of 1.8 eV,

significantly increasing visible-light absorption and photocatalytic performance.[22]

Zinc oxysulfide phase formation in the ZnO–ZnS system is another strongly promising route to band gap engineering. The solubility of ZnO and ZnS in two-component systems at high pressures and temperatures can be utilized to create oxysulfide phases with tailored electronic properties by design, thereby opening new avenues in the design of efficient photocatalysts.[3,23] The paper reports systematic studies of ZnOS structures developed through hydrothermal experiments and their application in hydrogen production. We investigate the relationship between synthesis parameters, structural properties, and functional performance with the goal of optimizing photocatalytic performance. Our research addresses major material synthesis challenges and provides insight into the relationship between the material's structure and properties, particularly in terms of their impact on the efficacy of hydrogen evolution. We also explore ways to maximize the stability and scalability of such materials for actual use.[32]

2. Materials and methods

2.1 Chemicals

All chemicals used in this study were analytical grade and were used without further purification. Zinc acetate dihydrate ($Zn(CH_3CO_2)_2 \cdot 2H_2O$, 5 g) and thiourea (5 g) were procured from Sigma-Aldrich. Urea and ammonia solutions were also employed for deposition on glass substrates. Distilled water was used throughout as a solvent to minimize the level of interference caused by impurities.

2.2 Preparation method

A schematic illustration of the hydrothermal synthesis and post-treatment process is presented in Fig. 1. The process begins with individual preparation of precursor solutions of $Zn(CH_3CO_2)_2 \cdot 2H_2O$ and thiourea in distilled water and controlled heating inside a Teflon-lined autoclave. The powders formed are collected after cooling, washed, dried, and optionally annealed at elevated temperatures to enhance crystallinity.

For ZnOS-1, zinc acetate dihydrate was dissolved in 40 mL of distilled water and stirred at room temperature for 1 h. Meanwhile, thiourea was dissolved in another 40 mL of distilled water at 30 °C for 1 h. The two solutions were then combined, maintaining a 1:1 mass ratio to achieve a total volume of 80 mL, and stirred for an additional hour to achieve homogeneity. The mixed solution was transferred into a 30 mL Teflon-lined autoclave and heated at 200 °C for 24 h. The autoclave was subsequently allowed to cool down to room temperature spontaneously after the reaction, and the pH of the solution was determined to be 5, a neutral medium. The synthesized powders were obtained by centrifugation at 5000 rpm for 5 minutes at 25 °C, washed with ethanol and distilled water, and oven-dried at 60 °C for 3 h. The sample was then dried and divided into two portions, one of which was annealed for 2 h at 500 °C. The same experiment was done with smaller amounts of precursors for ZnOS-2. Here, 1 g of zinc acetate dihydrate and 1 g of thiourea were dissolved separately in 50 mL of distilled water.

The deposition reaction was allowed to occur at 180 °C for 18 h, and the resulting powders were then annealed at 350 °C for 2 h. This sample was then characterized by scanning electron microscopy (SEM), X-ray diffraction (XRD), and Fourier transform infrared (FTIR) spectroscopy. For ZnOS-Glass film, the synthetic method was optimized for glass substrate deposition. Glass substrates (20 × 20 mm) were cleaned with acetone and methanol in an ultrasonic bath, and then distilled water was used to wash them. Deposition was carried out by dissolving 0.55 g (0.05 M) of zinc acetate dihydrate and 0.2 g (0.05 M) of thiourea in 50 mL of distilled water for both precursors. Additionally, a 10% urea solution (2.5 g urea in 25 mL of distilled water) and 25 mL of ammonia solution were added to the reaction bath. After synthesis, the synthesized ZnOS-Glass film was annealed in an oven at 400 °C for 30 min. The hydrothermal method employed here is highly reputed for synthesizing high-quality nanomaterials under relatively mild conditions.[33]

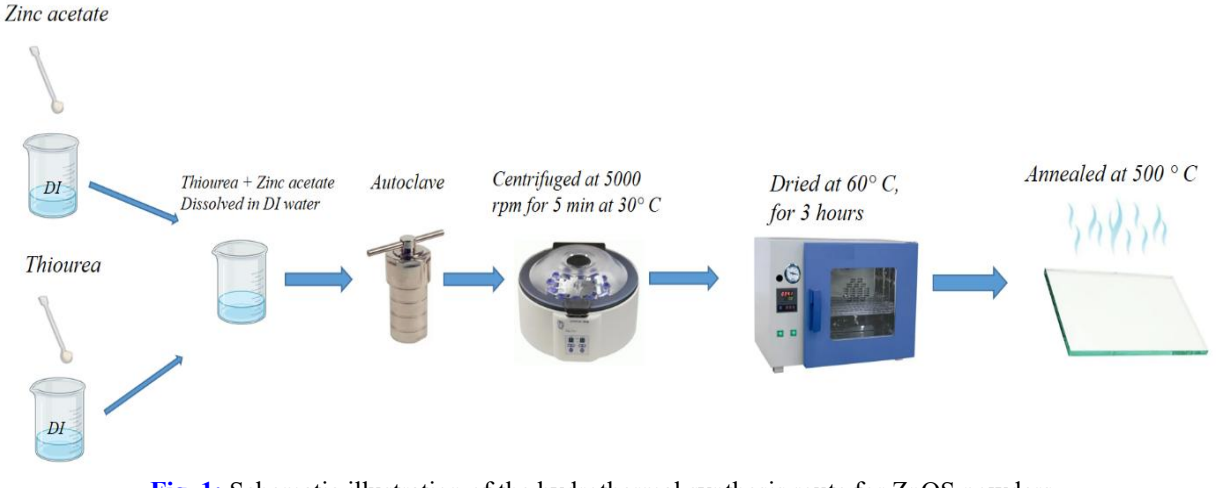

Fig. 1: Schematic illustration of the hydrothermal synthesis route for ZnOS powders.

2.3 Materials characterization

An array of sophisticated analysis techniques was employed to characterize the structural, compositional, and optical properties of the products. For ZnOS-1, SEM and energy-dispersive X-ray (EDS) analysis were employed to examine the surface morphology and determine the elemental composition, as indicated in Figs. 1 and 2. ZnOS-2 was examined by XRD to identify its crystallographic structure and phase purity, and FTIR spectroscopy was employed to investigate chemical bonding and identify functional groups; the corresponding results are indicated in Figs. 3-5. For ZnOS-Glass film, deposited on glass substrates, other optical characterization techniques were used. The optical properties were investigated using ultra-violet-visible (UV-Vis) absorbance spectroscopy, and Raman spectroscopy provided details on the nature and type of bonding and vibrational modes of the film. These, along with further SEM, XRD, and FTIR measurements, are presented in Figs. 6-10.

3. Results and discussion

3.1 Morphological and compositional analysis of ZnOS-1

Fig. 2(A) is the surface of ZnOS-1 before annealing, with spherical particles that are uniformly sized but have a rough surface. The particles are more rounded in some areas, while others exhibit flatter surfaces. The scale bar indicates the particles are approximately the size of microns. In Fig. 2(B), the surface after annealing reveals that the particles remain spherical but are smoother and more uniform. The roughness observed in the first image is less pronounced due to sintering or particle fusion during annealing, resulting in a smoother surface. The particle size distribution remains unchanged, but the surface texture is significantly improved. The preparation method involved applying a conductive carbon adhesive tape and then coating the ZnOS-1 with gold-palladium to make it conductive for SEM imaging. A 10 nm thick coating with a 60/40 ratio is suitable for providing conductivity while not covering the surface features.

As seen in Fig. 2, the surface morphology before annealing exhibits a "flower " structure, with a zinc oxide (ZnO) sphere inside zinc sulfide (ZnS). EDS spectra contain peaks for Zinc (Zn), Oxygen (O), and Sulfur (S), which are expected due to the presence of ZnO and ZnS. For Fig. 2A, the Oxygen peak is extremely high, while for Fig. 2B, it is not quite as high. This suggestion resulted in decreased oxygen content, likely due to enhanced oxysulfide formation. The important point is that annealing caused a transition toward more oxysulfide from more ZnO, as evidenced by the decrease in the O peak and the alteration of the Zn and S peaks. This agrees with the observed morphological transformation, where the surface becomes more crystalline and spherical. The EDS spectra confirms the formation of a more crystalline phase of oxysulfide upon annealing (Fig. 3).

In Fig. 4, the elemental overlay superimposes to reveal the distributions of oxygen (red), sulfur (yellow), and zinc (green), which predominantly reflect an oxygen-rich surface representative of the ZnO-dominant phase prior to heat treatment. The individual elemental maps also reveal that the oxygen signal is the highest, followed by sulfur, which is the weakest, and zinc, which is homogenously distributed across the particles. These results are in line with the EDS spectra (Fig. 3A) and verify the original heterogeneity reported in the as-synthesized ZnOS-1 sample. Fig. 5 displays a more uniform distribution of oxygen, sulfur, and zinc, with the sulfur signal appearing more uniform and a general reduction in oxygen intensity. The individual maps confirm the heat treatment has caused the formation of a more homogeneous ZnOS phase, as observed by the greater uniformity and better Zn–S features compared to the pre-annealed situation. This is consistent with the corresponding changes observed in the EDS spectra (Fig. 3A) and the more uniform surface morphology of the SEM images.

3.2 Crystallographic and chemical analysis of ZnOS-2

XRD spectrum was obtained using a Rigaku instrument with Cu Kα radiation (λ = 0.154 nm) over a range of 10–90°. Fig. 6 presents the XRD pattern of ZnOS powders with well-resolved diffraction peak match well the sphalerite (cubic)

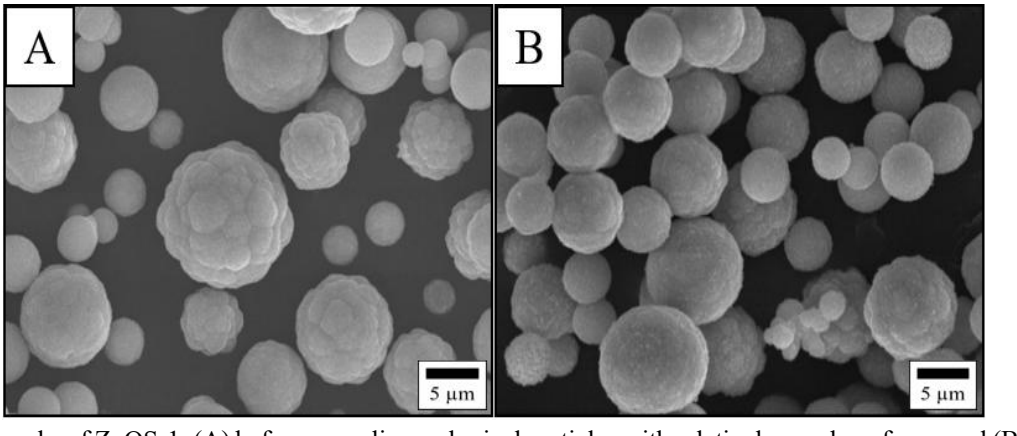

Fig. 2: SEM micrographs of ZnOS-1: (A) before annealing, spherical particles with relatively rough surfaces, and (B) after annealing, revealing smoother and more homogenized spheres.

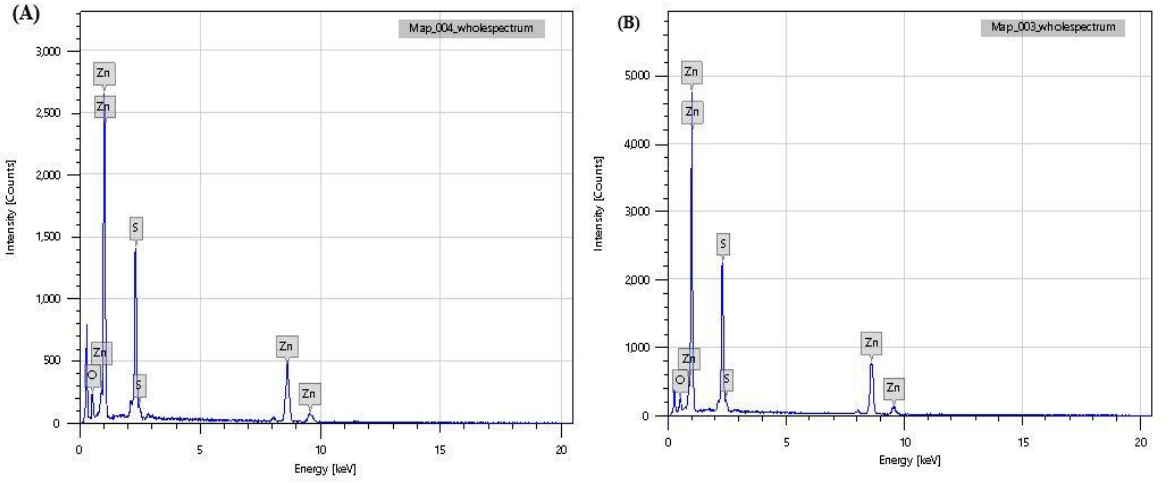

Fig. 3: EDS spectra of ZnOS-1: (A) before annealing, showing intense Zn, O, and S peaks and a very intense oxygen signal, and (B) after annealing, with reduced oxygen intensity and enhanced oxysulfide formation.

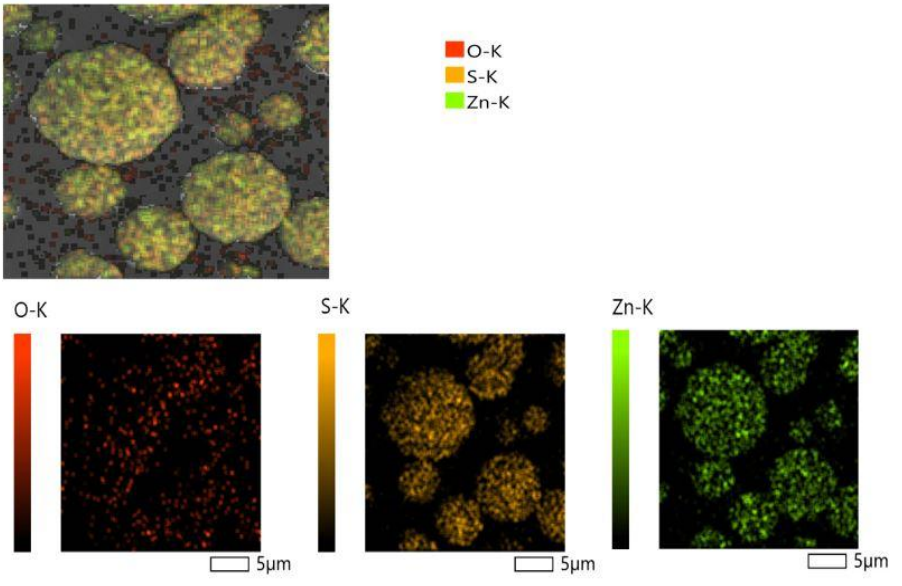

Fig. 4: EDS mapping of ZnOS-1 powder before annealing.

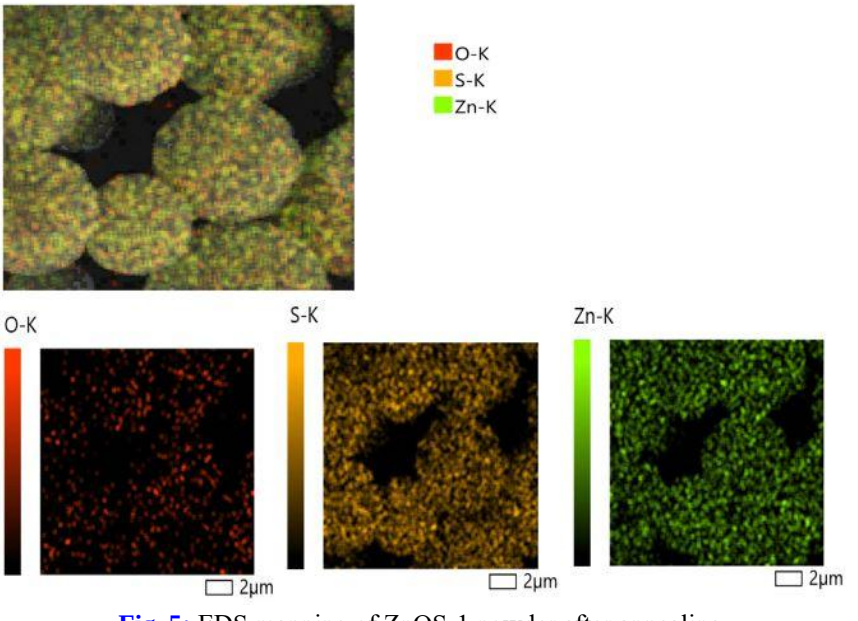

Fig. 5: EDS mapping of ZnOS-1 powder after annealing.

ZnS reference pattern (JCPDS 05-0566) indexed to the planes. The sharp and intense reflections confirm high crystallinity, and fine shifts in the peak positions indicate the partial incorporation of oxygen to achieve ZnOS. The crystallite size D was estimated using the Debye-Scherrer equation in Eq. (1):[34]

$$D = K\lambda/\beta cos\theta \quad (1)$$

where $K = 0.95$ is the shape factor, $\lambda = 0.154\,nm$ is the wavelength of the X-ray source, β is the full width at half maximum (FWHM) of the peak, and θ is the diffraction angle corresponding to the peak intensity.

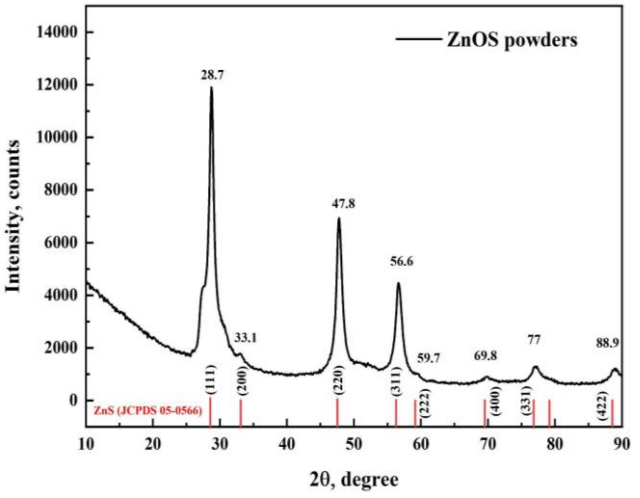

Fig. 6: XRD pattern of ZnOS-2 powders, showing characteristic diffraction peaks at 2θ values of 28.6, 47.8, and 56.6°, indicative of its crystalline structure.

The FTIR spectrum of ZnOS powder, shown in Fig. 7, exhibits intense transmittance ranging from 60% to 100% in the range of 4000–500 cm^{-1}, indicating optical clarity in this region of the spectrum. The occurrence of typical absorption at 1000–900 cm^{-1} is indicative of Zn–O stretching vibration, and the steep fall at 500 cm^{-1} is indicative of Zn–S bonds. The smooth spectrum with few peaks in the higher wavenumber area (4000–1500 cm^{-1}) ensures the purity of the ZnOS-2, i.e., the absence of organic impurities or hydroxyl groups. The SEM of the surface morphology of ZnOS-2 and ZnOS Glass film reveals clusters of spherical powders of varied sizes, between approximately 1 and 5 µm (Figs. 8 and 9). Similar to ZnOS-1, sulfide morphologies occur as surface coverages on spherical zinc oxides.

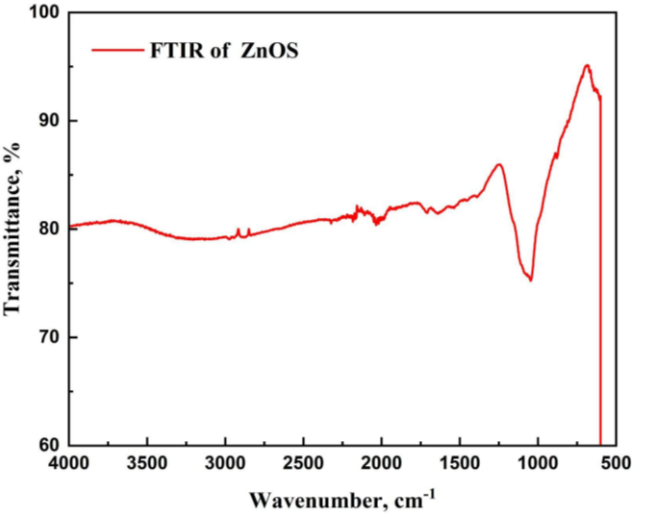

Fig. 7: FTIR spectrum of ZnOS-2, illustrating the transmittance profile and characteristic vibrational peaks associated with its functional groups.

3.3 Optical and structural properties of the ZnOS-glass film

Fig. 10 shows the UV-Vis absorbance spectrum of ZnOS films grown on glass before and after annealing, measured between 300 nm and 800 nm. The as-deposited sample exhibits a reduced absorption at the near-UV range, whereas the annealed film has an enhanced absorbance peak near 350 nm. Such increased absorption after heat treatment can be attributed to increased crystallinity, the formation of defect states, or a slight decrease in the band gap, which are all responsible for increased visible-light harvesting.

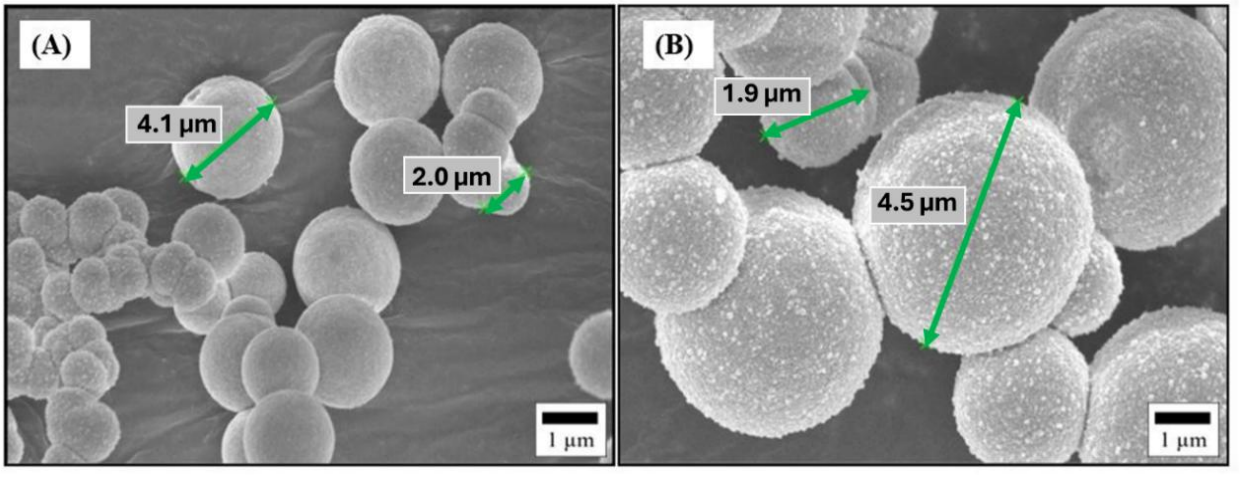

Fig. 8: SEM micrographs of ZnOS-2, displaying spherical particles with comparatively homogeneous particle size distribution (A) and textured morphology (B).

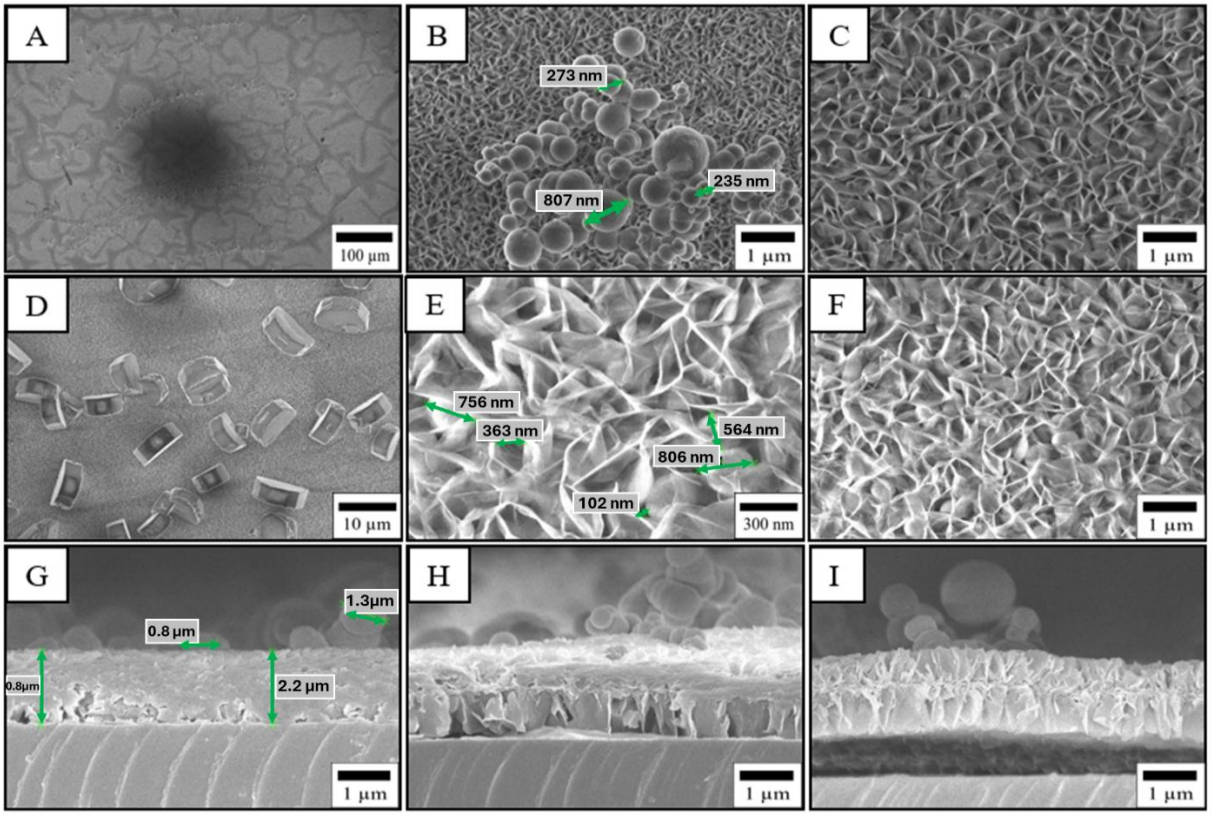

Fig. 9: SEM images of ZnOS after annealing on a glass substrate, showing surface morphology at different magnifications (A–F) and SEM cross-section images illustrating the film thickness and structural features (G–I).

The findings agree with previous research on similar materials. For instance, Arsad *et al*.[35] found that annealing ZnS thin films enhanced optical absorption and led to structural changes due to increased crystallinity and defect formation. The enhanced absorption characteristic at around 350 nm after annealing indicates that heat treatment effectively alters the electronic characteristics of the material, thereby improving the performance of devices that utilize optical absorption.

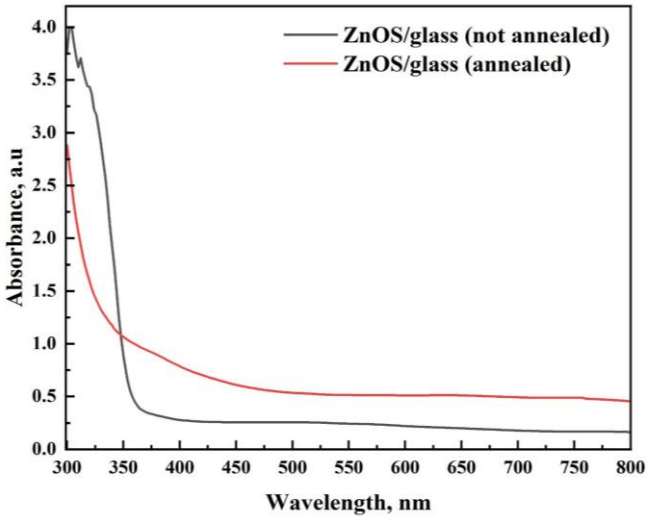

Fig. 10: UV-Vis absorbance spectra of the ZnOS-glass film, comparing the as-deposited and annealed states over the 300-800 nm range.

To establish the structural and optical characteristics of ZnOS films deposited on glass substrates, a suite of complementary analytical methods was employed. Fig. 11 is the XRD pattern of the ZnOS film. The broad features, approximately centered between 20–40° and 50–70° (2θ), suggest that the film is predominantly amorphous or composed of very small crystalline domains. This is characteristic of ZnOS materials under mild growth conditions, where mixed oxide/sulfide phases or incomplete crystallization may lead to lower long-range order. These general properties suggest a mixture of ZnS and ZnO phases within the ZnOS matrix. Annealing has been observed to enhance crystallinity by providing heat energy that facilitates atomic reorganization, often resulting in narrower and more intense diffraction peaks.[36]

The Raman spectrum in Fig. 12 shows distinct differences between the annealed and non-annealed ZnOS films. The spectrum shows sharp and strong peaks, particularly at around 1100 cm^{-1}, prior to annealing, which are typical vibrations of zinc oxysulfide structures. The peaks become broader and weaker after annealing, indicating the structural transformation caused by the annealing treatment. The shift of the peaks from 1100 cm^{-1} to 1000 cm^{-1} reveals the further oxidation of the structure, with sulfur atoms being partially replaced by oxygen. All these modifications are accompanied by improved crystal quality and a reduction in defect density, which are typical outcomes of thermal annealing for similar materials.[37]

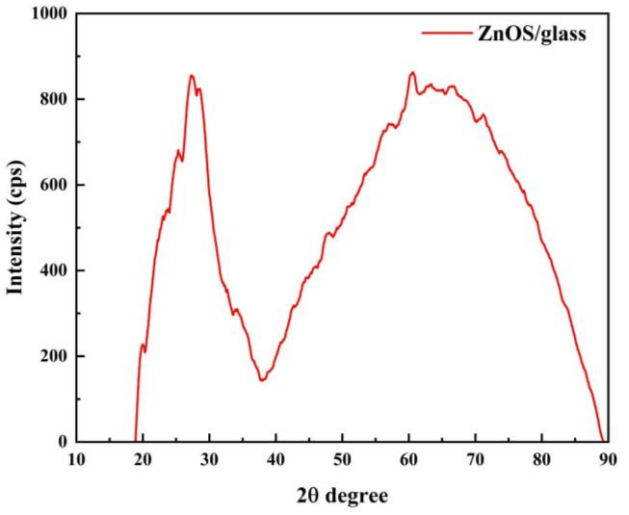

Fig. 11: XRD spectrum for ZnOS-Glass film.

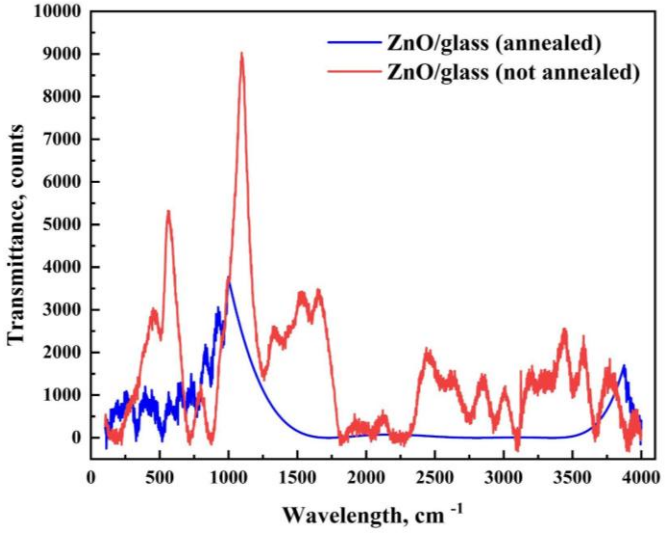

Fig. 12: Raman spectrum of ZnOS glass film before and after annealing.

Fig. 13 is the FTIR spectrum of the annealed ZnOS thin film (ZnOS-Glass film) in the mid-infrared region (400–4000 cm^{-1}). The presence of a strong absorption band at approximately 1000 cm^{-1} usually points to oxysulfide (Zn–O–S) or metal–oxygen–sulfur vibrational modes, and a peak around 450 cm^{-1} is caused by Zn–S stretching. Glass substrates, however, typically contain broad Si–O–Si bands between 900 and 1200 cm^{-1}. Hence, the presence and intensity of such Zn–O–S and Zn–S peaks are a definite indication that S and Zn are present in the film.

Upon annealing, such infrared (IR) absorption bands may alter or vary in intensity due to changes in bonding, crystallinity, or phase segregation. For instance, enhanced crystallinity would narrow and intensify peaks, and more oxidation could lead to shifts in the main absorption features to higher wavenumbers. Tracking these trends over a sequence of annealing temperatures and times is helpful in maximizing film quality and ensuring that the final material composition is as predicted for the application in optoelectronic devices or sensors.[38]

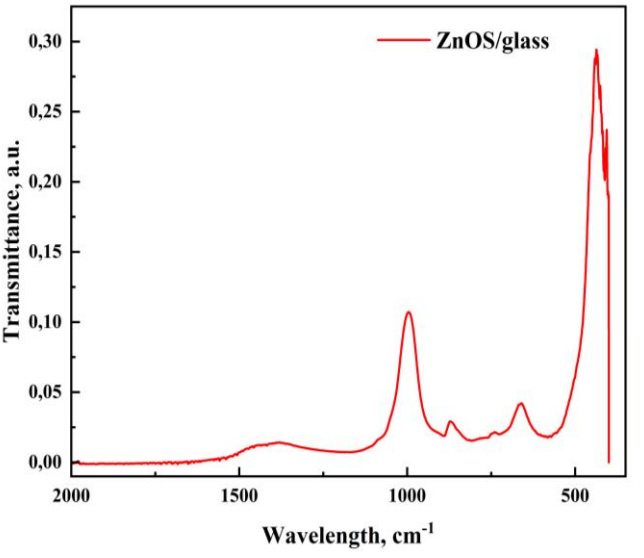

Fig. 13: FTIR spectrum of ZnOS/glass, showing characteristic vibrational peaks corresponding to functional groups and structural features of the material.

Collectively, the information gathered from XRD, Raman, and FTIR spectroscopic findings suggests that annealing plays a key role in promoting structural order and modulating the optical properties of ZnOS thin films, thereby paving the way for optimizing such films for advanced optoelectronics and solar technologies.

4. Conclusion

This research fully explored the hydrothermal synthesis of ZnOS architectures and their photocatalytic performance as efficient photocatalysts for hydrogen evolution. Our findings illustrate that synthesis conditions, such as precursor ratios, reaction temperature, and annealing conditions, are crucial in controlling the morphology, crystallinity, and optical properties of ZnOS materials. ZnOS powders (ZnOS-1 and ZnOS-2) showed uniform spherical particles with noticeable morphological changes upon annealing. SEM images revealed that annealing smoothened surface roughness through sintering or fusion of particles, and XRD patterns revealed that the heat treatment enhanced crystallinity by promoting the formation of a well-ordered, mixed ZnO–ZnS phase. EDS and FTIR analysis also established the shift in composition from nearly pure ZnO to a compound dominated by oxysulfides.

The ZnOS Glass film also exhibited improved optical properties upon annealing. The UV-Vis absorbance spectra showed a remarkable increase in absorbance around 350 nm, indicating that annealing facilitated not only an enhancement in crystallinity but also the effective tailoring of the electronic structure, presumably due to the creation of defect states or the narrowing of the bandgap. These are directly related to the proven improvement in photocatalytic activity. The successful

deposition of ZnOS on glass substrates demonstrates the versatility of the hydrothermal synthesis process, highlighting its suitability for applications in integrated optoelectronic devices and large-scale water-splitting cells for hydrogen generation. The enhanced visible light charge separation and absorption of the ZnOS heterostructures demonstrate the heterostructures' capability to outcompete conventional photocatalysts, such as TiO_2 and bare ZnO, in water splitting systems.

Building on these promising results, further optimization of hydrothermal conditions, specifically reaction time, precursor concentration, and annealing temperature, can achieve even greater control over the ZnOS phase composition and crystallinity. Research into varying annealing atmospheres (*e.g.*, inert or reducing) can also achieve more stable and defect-engineered structures. Research into techniques such as lanthanide doping or heterojunction formation can also fine-tune the band gap to better visible light absorption. These modifications may also improve the efficiency of charge separation and, hence, the rate of photocatalytic hydrogen evolution. To bridge the gap between laboratory experiments and actual applications, future studies need to focus on addressing the scalability of the synthesis procedure and the long-term stability of ZnOS photocatalysts under practical conditions.

Long-term durability testing under extended light and operating stress will be necessary for commercialization. Advanced mechanistic studies, combined with in situ characterization techniques (*e.g.*, synchrotron X-ray diffraction, time-resolved spectroscopy), can further clarify the phase transformation mechanisms and the roles of defects in ZnOS photocatalytic activity. Hydrothermal synthesis of ZnOS materials is a promising approach for designing tunable, high-efficiency photocatalysts for the production of green hydrogen. The knowledge gained from this study unlocks paths to further advancement in the engineering and material design process, which can ultimately enable the application of clean energy technologies.

Acknowledgement

This research was supported by the Science Committee of the Ministry of Science and Higher Education of the Republic of Kazakhstan (Grant No. AP23488359). This work has been also supported by the Targeted program of the Science Committee of the Ministry of Science and Higher Education of the Republic of Kazakhstan (Grant No. BR21882439).

Conflict of Interest

There is no conflict of interest.

Supporting Information

Not applicable.

References

[1] S. Wongsakulphasatch, S. Ratchahat, P. Kim-Lohsoontorn, W. Kiatkittipong, N. Weeranoppanant, M. Chanthanumataporn, S. Charojrochkul, N. Laosiripojana, S. Assabumrungrat, Hydrogen generation from fossil sources, in Hydrogen Production, Elsevier, 2024, 232-245, ISBN 978-0-323-96022-9.

[2] M. Abubakr, S. Shahid, I. Arman, A review on hydrogen production technologies and its future demand, arxiv preprint arxiv: 2410.08154, 2024, doi: 10.48550/arxiv.2410.08154.

[3] A. N. Salak, O. V. Ignatenko, A. L. Zhaludkevich, A. D. Lisenkov, M. Starykevich, M. L. Zheludkevich, M. G. S. Ferreira, High-pressure zinc oxysulphide phases in the ZnO-ZnS system, *Physica Status Solidi (a)*, 2015, **212**, 791-795, doi: 10.1002/pssa.201431820.

[4] X. Chen, C. Lin, L. Lai, M. Liu, K. Zheng, S. Li, H. Li, Collaborative hydrothermal and calcination fabrication of ZnOS heterostructures for visible-light-driven H_2 production, *Physical Chemistry Chemical Physics*, 2023, **25**, 3617-3621, doi: 10.1039/d2cp05351a.

[5] Y. Zhang, X. Bo, T. Zhu, W. Zhao, Y. Cui, J. Chang, Synthesis of TiO_2-ZnO n-n heterojunction with excellent visible light-driven photodegradation of tetracycline, *Nanomaterials*, 2024, **14**, 1802, doi: 10.3390/nano14221802.

[6] Lalhriatzuala, P. Agarwal, High-pressure solvothermal route to synthesize II–VI sulfide compounds, *Applied Physics A*, 2021, **127**, 83, doi: 10.1007/s00339-020-04237-3.

[7] O. Mauit, D. Caffrey, A. Ainabayev, A. Kaisha, O. Toktarbaiuly, Y. Sugurbekov, G. Sugurbekova, I. V. Shvets, K. Fleischer, Growth of ZnO: Al by atomic layer deposition: deconvoluting the contribution of hydrogen interstitials and crystallographic texture on the conductivity, *Thin Solid Films*, 2019, **690**, 137533, doi: 10.1016/j.tsf.2019.137533.

[8] M. Y. Chia, W. S. Chiu, N. H. M. Hasnan, P. S. Khiew, M. A. A. Hamid, Hydrothermal growth of 1D ZnO nanorods thin films for hydrogen gas production through water splitting reaction, *Solid State Phenomena*, 2017, **264**, 95-98, doi: 10.4028/www.scientific.net/ssp.264.95.

[9] A. Gupta, A. Kumar, Surbhi, M. P. Srivastava, D. K. Rana, Facile growth of zinc oxysulfide nano thin film-based visible light photosensor by hydrothermal method, *ECS Journal of Solid State Science and Technology*, 2024, **13**, 077003, doi: 10.1149/2162-8777/ad6036.

[10] Z. Yao, Y. He, Q. Xia, H. Wei, Z. Jiang, Hydrothermal synthesis of a uniform sub-micrometer-spherical $Zn_{0.83}Cd_{0.17}S$ photocatalyst with high activity for photocatalytic hydrogen production, *RSC Advances*, 2016, **6**, 51997-52003, doi: 10.1039/c6ra12556e.

[11] R. Shan, J. Yi, J. Zhong, S. Yang, Effect of sulphur pressure on properties of ZnS thin film prepared by chemical bath deposition technique, *Journal of Materials Science: Materials in Electronics*, 2019, **30**, 13230-13237, doi: 10.1007/s10854-019-01686-2.

[12] X. Jian, J. Li, L. He, H. Li, M. Zhang, P. Zhang, H. Lin, Severe plastic deformation for advanced electrocatalysts for electrocatalytic hydrogen production, *Materials Transactions*, 2023, **64**, 1515-1525, doi: 10.2320/matertrans.mt-mf2022011.

[13] A. O. M. Maka, M. Mehmood, T. N. Chaudhary, Green hydrogen revolution and its pathway towards sustainable development, *Clean Energy*, 2025, **9**, 124-131, doi: 10.1093/ce/zkae106.
[14] R. Fan, Current hydrogen production methods and their economic and environmental analysis, *Highlights in Science, Engineering and Technology*, 2024, **116**, 75-80, doi: 10.54097/avdxz945.
[15] Z. Qian, Hydrogen: production, applications, and challenges in sustainable energy systems, *Highlights in Science, Engineering and Technology*, 2024, **119**, 10-15, doi: 10.54097/bhm5qc18.
[16] S. O. Akpasi, I. M. Smarte Anekwe, E. K. Tetteh, U. O. Amune, S. I. Mustapha, S. L. Kiambi, Hydrogen as a clean energy carrier: advancements, challenges, and its role in a sustainable energy future, *Clean Energy*, 2025, **9**, 52-88, doi: 10.1093/ce/zkae112.
[17] S. Chatterjee, A. Palui, S. Chongdar, S. Roy, A. Ghosh, A. Bhaumik, Transformation of wurtzite ZnO to a new triclinic nanoporous ZnO phase *via* hydrothermal treatment with metformin for designing proton conducting material, *Chemistry - An Asian Journal*, 2021, **16**, 2261-2266, doi: 10.1002/asia.202100601.
[18] X. Xue, T. Wang, X. Jiang, J. Jiang, C. Pan, Y. Wu, Interaction of hydrogen with defects in ZnO nanoparticles-studied by positron annihilation, Raman and photoluminescence spectroscopy, *CrystEngComm*, 2014, **16**, 1207, doi: 10.1039/c3ce42202j.
[19] S. Akrami, P. Edalati, M. Fuji, K. Edalati, High-pressure torsion for highly-strained and high-entropy photocatalysts, *KONA Powder and Particle Journal*, 2024, **41**, 123-139, doi: 10.14356/kona.2024003.
[20] H. Razavi-Khosroshahi, M. Fuji, Development of metal oxide high-pressure phases for photocatalytic properties by severe plastic deformation, *Materials Transactions*, 2019, **60**, 1203-1208, doi: 10.2320/matertrans.mf201916.
[21] Y. Shundo, T. Tam Nguyen, S. Akrami, P. Edalati, Y. Itagoe, T. Ishihara, M. Arita, Q. Guo, M. Fuji, K. Edalati, Oxygen vacancy-rich high-pressure rocksalt phase of zinc oxide for enhanced photocatalytic hydrogen evolution, *Journal of Colloid and Interface Science*, 2024, **666**, 22-34, doi: 10.1016/j.jcis.2024.04.010.
[22] H. Razavi-Khosroshahi, K. Edalati, J. Wu, Y. Nakashima, M. Arita, Y. Ikoma, M. Sadakiyo, Y. Inagaki, A. Staykov, M. Yamauchi, Z. Horita, M. Fuji, High-pressure zinc oxide phase as visible-light-active photocatalyst with narrow band gap, *Journal of Materials Chemistry A*, 2017, **5**, 20298-20303, doi: 10.1039/c7ta05262f.
[23] H. Abdullah, N. S. Gultom, D. H. Kuo, H. Shuwanto, Progress of Zn(O, S) based nanoparticles for hydrogen evolution reaction and its application for hydrogenation reaction, 2021 IEEE International Conference on Health, Instrumentation & Measurement, and Natural Sciences (InHeNce), July 14-16, Medan, Indonesia, IEEE, 2021, 1-6, doi: 10.1109/InHeNce52833.2021.9537208.
[24] X. Chen, C. Lin, L. Lai, K. Zheng, S. Li, Y. Chen, H. Li, Collaboratively hydrothermal and calcination fabrication of ZNOS heterostructures for visible-light-driven H_2 production, *Physical Chemistry Chemical Physics*, 2022, **25**, 3617-3621, doi: 10.21203/rs.3.rs-2104847/v1.
[25] D. Buckley, A. Lonergan, C. O'Dwyer, ZnO-based semiconductors and structures for transistors, optoelectronic devices and sustainable electronics, arXiv preprint arXiv: 2411.13304, 2024, doi: 10.48550/arxiv.2411.13304.
[26] A. Sivakumar, S. S. J. Dhas, A. I. Almansour, R. S. Kumar, N. Arumugam, S. A. Martin Britto Dhas, Spectroscopic assessment of shock wave resistance on ZnO nanorods for aerospace applications, *Journal of Inorganic and Organometallic Polymers and Materials*, 2021, **31**, 2553-2559, doi: 10.1007/s10904-020-01848-4.
[27] A. Segura, J. A. Sans, F. J. Manjón, A. Muñoz, M. J. Herrera-Cabrera, Optical properties and electronic structure of rock-salt ZnO under pressure, *Applied Physics Letters*, 2003, **83**, 278-280, doi: 10.1063/1.1591995.
[28] J. Pellicer-Porres, A. Segura, V. Panchal, A. Polian, F. Decremps, P. Dumas, High-pressure study of the infrared active modes in wurtzite and rocksalt ZnO, *Physical Review B*, 2011, **84**, 125202, doi: 10.1103/physrevb.84.125202.
[29] Z. Horita, Y. Tang, T. Masuda, K. Edalati, Y. Higo, In situ synchrotron high-pressure X-ray analysis for ZnO with rocksalt structure, *Materials Transactions*, 2023, **64**, 1585-1590, doi: 10.2320/matertrans.mt-mf2022036.
[30] J. E. Jaffe, A. C. Hess, Hartree-Fock study of phase changes in ZnO at high pressure, *Physical Review B*, 1993, **48**, 7903-7909, doi: 10.1103/physrevb.48.7903.
[31] V. I. Levitas, M. Javanbakht, Phase transformations in nanograin materials under high pressure and plastic shear: nanoscale mechanisms, *Nanoscale*, 2014, **6**, 162-166, doi: 10.1039/c3nr05044k.
[32] A. A. Markhabayeva, Z. K. Kalkozova, R. Nemkayeva, Y. Yerlanuly, A. S. Anarova, M. A. Tulegenova, A. T. Tulegenova, K. A. Abdullin, Construction of a ZnO heterogeneous structure using Co_3O_4 as a co-catalyst to enhance photoelectrochemical performance, *Materials*, 2024, **17**, 146, doi: 10.3390/ma17010146.
[33] R. S. Desai, V. S. Jadhav, P. S. Patil, D. S. Dalavi, Recent advances in hydrothermally and solvothermally grown Co_3O_4 nanostructures for electrochemical energy storage (EES) applications: a brief review, *Materials Advances*, 2024, **5**, 920-960, doi: 10.1039/d3ma00806a.
[34] M. Sivagami, I. Asharani, Phyto-mediated Ni/NiO NPs and their catalytic applications-a short review, *Inorganic Chemistry Communications*, 2022, **145**, 110054, doi: 10.1016/j.inoche.2022.110054.
[35] A. Z. Arsad, M. S. Bahrudin, N. A. Arzaee, M. N. A. Rahman, C. F. Chau, S. F. Abdullah, A. W. Mahmood Zuhdi, Zinc sulfide thin films deposited by chemical bath: Tuning consideration of structural, optical band gap, and electrical properties for CIGS solar cells application, *Ceramics International*, 2024, **50**, 11776-11786, doi:

10.1016/j.ceramint.2024.01.082.
[36] M. Jothibas, S. Johnson Jeyakumar, C. Manoharan, I. Kartharinal Punithavathy, P. Praveen, J. Prince Richard, Structural and optical properties of zinc sulphide nanoparticles synthesized *via* solid state reaction method, *Journal of Materials Science*: *Materials in Electronics*, 2017, **28**, 1889-1894, doi: 10.1007/s10854-016-5740-6.
[37] A. Baranowska-Korczyc, M. Kościński, E. L. Coy, B. F. Grześkowiak, M. Jasiurkowska-Delaporte, B. Peplińska, S. Jurga, ZnS coating for enhanced environmental stability and improved properties of ZnO thin films, *RSC Advances*, 2018, **8**, 24411-24421, doi: 10.1039/c8ra02823k.
[38] J. Yuvaloshini, R. Shanmugavadivu, G. Ravi, Effect of annealing on optical and structural properties of ZnS/MnS and MnS/ZnS superlattices thin films for solar energy application, *Optik*, 2014, **125**, 1775-1779, doi: 10.1016/j.ijleo.2013.09.031.